Self-evolved Hydrogen Peroxide Boosts Photothermal-promoted Tumor-specific Nanocatalytic Therapy

Shanshan Gao,[a,b] Xiangyu Lu,[a,b] Piao Zhu,[a,b] Han Lin,[a,b] Luodan Yu,[a] Heliang Yao,[a] Chenyang Wei,[a] Yu Chen*[a] and Jianlin Shi*[a]

[a]State Key Laboratory of High Performance Ceramics and Superfine Microstructure, Shanghai Institute of Ceramics, Chinese Academy of Sciences, Shanghai 200050, P. R. China.
E-mail: chenyu@mail.sic.ac.cn (Y. Chen); jlshi@mail.sic.ac.cn (J. Shi).

[b]University of Chinese Academy of Sciences, Beijing 100049, P. R. China.

A: Experimental Section

1. Materials and Reagents

The Nb_2AlC ceramic powder was obtained from Forsman Scientific Co., Ltd. (Beijing, China). Ammonia solution (NH_4OH, 28 wt%), hydrochloric acid (HCl) aqueous solution (37 wt%), calcium hydroxide ($Ca(OH)_2$), methanol, ethanol were obtained from Sinopharm Chemical Reagents Co., Ltd. (Shanghai, China). Hydrofluoric acid (HF) aqueous solution (50 wt%) was obtained from Adamas Reagent Co., Ltd. (Shanghai, China). Ferrous sulfate ($FeSO_4 \cdot 7H_2O$), tetrapropylammonium hydroxide (TPAOH) aqueous solution (25 wt%) was obtained from J&K Scientific Co., Ltd. (Beijing, China). Hydrogen peroxide (H_2O_2) aqueous solution (30 wt%), polyvinylpyrrolidone (PVP, average MW 40000), fluorescein isothiocyanate (FITC), 2,7-dichlorofluorescin diacetate (DCFH-DA), (3-Aminopropyl)triethoxysilane (APTES), horseradish peroxidase (HRP) and 1,3,5-trimethylbenzene (TMB) were purchased from Sigma-Aldrich. Sodium phosphate dibasic ($NaHPO_4$) and citric acid (CA) were obtained from Shanghai Macklin Co., Ltd. The Nb_2AlC ceramic powder was purchased from Beijing Forsman Scientific Co., Ltd. All chemicals were used as received without further purification. Deionized water was used in all synthetic experiments.

2. Synthesis of Nb_2C Nanosheets (MXenes)

The Nb_2AlC ceramic powder (10 g) was dispersed and stirred in HF aqueous solution (60 mL) for 48 h at room temperature. Then, the precipitate was collected by high-speed centrifugation (20000 rpm, 15 min), and washed with ethanol and water for several times. The precipitate was dispersed and stirred in TPAOH aqueous solution (60 mL, 25 wt %) for 48 h at room temperature. Finally, the raw Nb_2C nanosheets were collected by centrifugation and washed three times with ethanol to remove the residual reactants.

3. Synthesis of Nb_2C-Iron Oxide (Nb_2C-IO) Composite Nanosheets

Nb_2C nanosheets were prepared by the chemical co-precipitation method.[1] Nb_2C nanosheets (1 mg mL^{-1}) was firstly dispersed into deionized water and treated with sonication for 30 min to produce stable Nb_2C aqueous solution with small particle sizes. For Fe_3O_4 loading, ammonia solution (1 mL) was added into the Nb_2C solution (10 mL) under magnetic stirring. Then, the fresh $FeSO_4 \cdot 7H_2O$ solution (0.5 M, 0.1 mL) was added into above solution dropwise under vigorous stirring. The reaction was continued for 10 min at room temperature under magnetic stirring. Finally, the resulting product was obtained by centrifugation and washed three times with water to remove the residual reactants.

4. Synthesis of CaO_2 Nanoparticles

PVP (6.0 g) was dissolved into 12 mL deionized water and treated with sonication until dissolving absolutely. Then, $Ca(OH)_2$ (0.6 g) was added into the above solution and stirred for 20 min, followed by adding H_2O_2 (4.0 mL) dropwise under vigorous stirring. After the reaction was continued for 15 min, and stable CaO_2 nanoparticles were formed. Finally, the products were separated by centrifuging and washed with deionized water and anhydrous ethanol.

5. Synthesis of Nb_2C-IO-CaO_2 Nanosheets

Nb_2C-IO composite nanosheets were aminated with alkoxysilanes *via* silylation reaction according to the previous report.[2] Briefly, APTES (1 mL) were added to the Nb_2C-IO composite nanosheets (1 mg mL^{-1}, 20 mL) and stirred at 50 °C for 2 h to form the aminated Nb_2C-IO (Nb_2C-IO-NH_2). The obtained Nb_2C-IO-NH_2 composite nanosheets were further stirred with the CaO_2 NPs in anhydrous ethanol for 24 h followed by centrifugation to obtain the resultant Nb_2C-IO-CaO_2 composite nanosheets.

6. Surface Modification

The as-synthesized Nb_2C-IO-CaO_2 composite nanosheets (20 mg) were dispersed into the PVP aqueous solution (1 mg mL^{-1}, 20 mL), followed by refluxed at 50 °C for 8 h. After collected by centrifugation and washed with ethanol, the precipitate of Nb_2C-IO-CaO_2-PVP composite nanosheets were obtained.

7. Material Characterization

Transmission electron microscopy (TEM) was conducted on a JEOL-2100F transmission electron microscope with the acceleration voltage of 200 kV. Scanning electron microscopy (SEM) images and element mapping scanning were acquired on a field-emission Magellan 400 microscope (FEI Company, USA). Dynamic light scattering (DLS) and zeta potential measurement were performed on a Zetasizer Nanoseries (Nano ZS90, Malvern Instrument Ltd.). UV-vis spectra absorbance spectra were measured on a UV-3600 Shimadzu UV-vis spectrometer. Fourier transform infrared spectroscopy (FT-IR) spectra were acquired on a Thermo Scientific Nicolet iS 10 FT-IR spectrometer. X-ray diffraction (XRD) experiment was conducted on a Rigaku D/MAX-2200 PC XRD system at Cu Kα (λ = 0.154056 nm). X-ray photoelectron spectroscopy (XPS) was performed on an ESCAlab250 (Thermal Scientific). Electron spin resonance (ESR) spectra were recorded by a Bruker EMX1598 spectrometer. Quantitative elemental analysis was conducted by an Agilent 725 inductively coupled plasma-optical emission spectrometry (ICP-OES, Agilent

Technologies, USA). The temperature change profiles and thermal images were obtained by an infrared thermal imaging system (FLIR^{TM} A325SC camera, USA). 1064 nm laser was generated from a high power multimode pump laser (Shanghai Connect Fiber Optics Company). Confocal laser scanning microscopy (CLSM) images were acquired by FV1000 (Olympus Company, Japan). Flow cytometry were obtained by a BD LSRFortessa flow cytometer (Becton, Dickinson and Company, USA) and analyzed by the Flowjo software.

8. Extinction Coefficient of Nb_2C-IO-CaO_2 Nanosheets

Firstly, the absorbance of Nb_2C-IO-CaO_2 nanosheets at varying concentrations (2.5, 5, 10, 20, 40 μg mL^{-1}) at 1064 nm was recorded from the UV-vis spectra. Then, the extinction coefficient ε of Nb_2C-IO-CaO_2 nanosheets was calculated by the Lambert-Beer Law known as A/L = εC, where A is the normalized adsorption intensity at 1064 nm, L is the path-length, and C is the concentration of Nb_2C-IO-CaO_2 nanosheets. The extinction coefficient (ε) of Nb_2C-IO-CaO_2 nanosheets at 1064 nm was calculated to be 18.8 L g^{-1} cm^{-1} by plotting the slope of linear fit against wavelength.

9. Photothermal Conversion Efficiency of Nb_2C-IO-CaO_2 Nanosheets

Photothermal performance of Nb_2C-IO-CaO_2 nanosheets was obtained and analyzed by irradiating Nb_2C-IO-CaO_2 nanosheets dispersion in an Eppendorf tube.

Following the modified method previously reported by Roper et al.[3], the energy balance for the whole system is

$$\sum_i m_i C_{p,i} \frac{dT}{dt} = Q_1 + Q_0 - Q_{Surr} \quad (1)$$

where m and Cp are the mass of solvent (water) and the heat capacity, T means solution temperature, and t is time. Q_1 is the energy input to the Nb_2C-IO-CaO_2 nanosheets, Q_0 is the energy input of the sample cell, and Q_{Surr} is the heat conduction away from the system.

The NIR laser-induced source term, Q_1 represents heat dissipated by electron-phonon relaxation of the plasmons on the Nb_2C-IO-CaO_2 nanosheets surface under the 1064 nm laser irradiation,

$$Q_1 = I\left(1 - 10^{-A_\lambda}\right)\eta \tag{2}$$

where I is incident laser power (mW), A_λ represents the absorbance of the Nb_2C-IO-CaO_2 nanosheets at 1064 nm, and η is the photothermal-conversion efficiency from incident NIR laser energy to thermal energy. Besides, Q_0 represents heat dissipated from light absorption of the sample cell itself, which was measured independently to be $Q_0 = \left(5.4 \times 10^{-4}\right)I$ using a sample cell containing pure water. $Q_{Surr}$is a temperature-dependent parameter, which is linear with the output of thermal energy:

$$Q_{Surr} = hS\left(T - T_{Surr}\right) \tag{3}$$

where h represents the heat-transfer coefficient, S represents the surface area of the container, T represents the solution temperature and T_{Surr}represents the temperature of the surroundings.

During the laser irradiation process, the heat input $(Q_1 + Q_0)$ is finite. The system temperature will reach a maximum value when the external heat flux by equation (3) equals to heat input *via* laser transduction given by equation (2):

$$Q_1 + Q_0 = Q_{Max} = hS\left(T_{Max} - T_{Surr}\right) \tag{4}$$

where Q_{Max} represents the conducting heat away from the system when the sample cell reaches the equilibrium temperature and T_{Max} is the maximum system temperature. The photothermal conversion efficiency (η) can be obtained by substituting equation (2) for Q_{input} into equation (4) and rearranging to get

$$\eta = \frac{hS(T_{Max} - T_{Surr}) - Q_0}{I\left(1 - 10^{-A_\lambda}\right)} \tag{5}$$

Thus, only the hS remains unknown for calculation of η. In order to obtain the hS, a dimensionless driving force temperature, θ is introduced, scaled using the maximum system temperature T_{Max}

$$\theta = \frac{T - T_{Surr}}{T_{Max} - T_{Surr}} \tag{6}$$

and a time constant of sample system τ_s

$$\tau_s = \frac{\sum_i m_i C_{p,i}}{hS} \tag{7}$$

which are substituted into the equation (1) and rearranged to yield

$$\frac{d\theta}{dt} = \frac{1}{\tau_s}\left[\frac{Q_1 + Q_0}{hS(T_{Max} - T_{Surr})} - \theta\right] \tag{8}$$

When the laser radiation ceases, $Q_1 + Q_0 = 0$ and the system cools, reducing the equation (8) to

$$dt = -\tau_s \frac{d\theta}{\theta} \tag{9}$$

Equation (9) can be solved using the initial condition θ = 1 and t = 0 to give

$$t = -\tau_s \ln \theta \tag{10}$$

Therefore, the time constant of heat transfer from the system was determined to be τ_s= 196.2 s at 1064 nm. In addition, according to equation (7), the hS can be determined with m = 0.3 g and C = 4.2 J g^{-1}. Substituting hS into equation (5), the 1064 nm laser e photothermal conversion efficiency (η) of Nb_2C-IO-CaO_2 nanosheets can be

calculated to be 32.1%.

10. Hydrogen Peroxide Detection Assay

The TMB reagent, in combination with HRP, was used to detect H_2O_2 generated from CaO_2 NPs. In the presence of HRP, TMB can react with H_2O_2 to produce the blue-colored oxidation product, oxTMB which possesses UV-vis absorption maxima at 370 nm and 652 nm. Na_2HPO_4-citric acid buffer solution (pH 5, 6.5, 7.4, 8.0) was prepared as the reaction buffer. TMB (1 mM) and HRP (0.1 unit mL^{-1}) were mixed in buffer solution at pH 6.5, followed by adding CaO_2 NPs of varied concentrations (0, 1, 2, 5, 10 μg mL^{-1}). The UV-vis absorption variation at 652 nm of the buffer solution was monitored using a microplate reader (SpectraMax M2, Molecular Devices, USA).

11. Catalytic Activities of Nb_2C-IO and Nb_2C-IO-CaO_2 Nanosheets

TMB was applied as substrates to investigate the catalytic activity of Nb_2C-IO and Nb_2C-IO-CaO_2 nanosheets. To investigate the effect of temperature, the Nb_2C-IO or Nb_2C-IO-CaO_2 nanosheets were incubated at different temperatures (25, 30, 35, 40, 45℃) or irradiated with 1064 nm laser of different power densities (0, 0.5, 1.0, and 2.0 W cm^{-2}) for 10 min. The steady-state kinetic catalytic activities of Nb_2C-IO and Nb_2C-IO-CaO_2 nanosheets were investigated by a microplate reader. The Michaelis-Menten kinetics model was applied to analyze the kinetic catalytic behaviors of Nb_2C-IO nanosheets.

12. Cell Culture

Murine breast cancer 4T1 cell line (4T1 cells) and human umbilical vein endothelial (HUVEC) cells were obtained from Cell Bank of Shanghai Institutes for Biological Sciences, Chinese Academy of Sciences. The cells were cultured in a humidified incubator (Thermo Fisher Scientific Inc. USA) with 5% CO_2 at 37°C in Dulbecco's Modified Eagle Medium (DMEM, GIBCO, Invitrogen) supplemented with 10% fetal bovine serum (FBS), penicillin (100 units mL^{-1}) and streptomycin (100 mg mL^{-1}). To simulate the acidic extracellular microenvironment in solid tumor,HCl was used to acidize the DMEM (pH 7.4) to pH 6.5.

13. *In Vitro* Cytotoxicity Measurements and Photothermal Ablation

In all cell and animal experiments, the Nb_2C-IO and Nb_2C-IO-CaO_2 were modified with PVP molecules for improved physiological stability and biocompatibility. The standard Cell Counting Kit-8 (CCK-8) assay (Sihai Bio-Tech Co., Ltd, Shanghai) was applied to evaluate the cytotoxicity of Nb_2C-IO-CaO_2 nanosheets. 4T1 cells or HUVEC cells were seeded (1×10^4 cells in 100 μL of DMEM per well) in 96-well microplates and allowed to adhere overnight, then the culture media were replaced by fresh DMEM containing different concentrations of Nb_2C-IO-CaO_2 nanosheets (0, 6.25, 12.5, 25, 25, 50, 100 and 200 ppm). After further incubation for 12 or 24 h, the culture media were replaced by FBS-free medium containing 10% CCK-8. After further co-incubation for 1 h, the cell proliferation was determined using the microplate reader by comparing the absorbance at 450 nm to the control group. The cytotoxicities of Nb_2C-IO nanosheets (0, 6.25, 12.5, 25, 50 and 100 ppm), CaO_2 NPs (0, 12.5, 25, 50, 100, 200, and 400 ppm), and H_2O_2 (0, 50, 100, 200, 300, 400, 500 and 1000 μM) were tested similarly.

To conduct the *in vitro* photothermal ablation of cancer cells, 4T1 tumor cells were seeded and allowed to adhere overnight. Then, the culture media were replaced by fresh DMEM (pH 7.4 or 6.5) containing Nb_2C-IO-CaO_2 nanosheets at varied concentrations (25, 50, 100, 150, 200 ppm). After further incubation for 6 h, the culture medium was replaced by fresh DMEM medium, followed by irradiation for 5 min under 1064 nm laser at varied power densities (0, 0.5, 1.0, and 1.5 W cm^{-2}). Finally, the CCK-8 assay was conducted to evaluate the cytotoxicity of Nb_2C-IO-CaO_2 nanosheets under 1064 nm laser.

14. Intracellular Endocytosis Analysis

The intracellular endocytosis analysis of Nb_2C-IO-CaO_2 nanosheets was conducted by flow cytometry. 4T1 cells were seeded (1×10^5 cells per well) in 6-well plates and allowed to adhere overnight. Then, the culture media were replaced by FITC-labeled Nb_2C-IO-CaO_2 nanosheets in DMEM (50 ppm, 1 mL). After co-incubation for 0, 30 min, 1 h, 2 h, 3 h, 4 h, and 6 h, the 4T1 cells were transferred into the test tube and flow

cytometry analysis was performed to evaluate the intracellular endocytosis of FITC-labeled Nb_2C-IO-CaO_2 nanosheets.

15. Intracellular ROS Evaluation

The intracellular ROS evaluation of Nb_2C-IO-CaO_2 nanosheets with or without the irradiation of 1064 nm laser was conducted by flow cytometry and CLSM.

For flow cytometry test, 4T1 cells were seeded (1×10^5 cells per well) in 6-well plates and allowed to adhere overnight. After various treatments of H_2O_2 (100 μM), Nb_2C-IO (50 ppm) or Nb_2C-IO-CaO_2 nanosheets (50 ppm) at pH 7.4 or 6.5 for 4 h, with or without the irradiation of 1064 nm laser (1.0 W cm^{-2}), the cells were stained by 1 mL DCFH-DA (10 μM in FBS-free DMEM) and further incubated for 30 min. The cells were then rinsed with phosphate-buffered saline (PBS) three times and transferred into the test tube, followed by detecting the fluorescence of DCF (λ_{ex} = 488 nm, λ_{em} = 525 nm) by flow cytometry analysis to determine the intracellular ROS level.

For CLSM observation, 4T1 cells were seeded (1×10^5 cells in 1 mL DMEM) in the CLSM-exclusive culture dish for 12 h to adhere. After various treatments, the culture medium was replaced by 1 mL DCFH-DA (10 μM in FBS-free DMEM) and incubated for 30 min, followed by washing with PBS three times. Before CLSM observation, cell nuclei was stained by 4',6-diamidino-2-phenylindole (DAPI, Beyotime Biotechnology) for 20 min. The quantitative analysis of the intracellular ROS production was conducted using Image J software.

16. *In Vitro* Flow Cytometric Apoptosis Assay

4T1 cells were seeded (1×10^5 cells per well) in 6-well plates and allowed to adhere overnight. After various treatments of H_2O_2 (100 μM), Nb_2C-IO (50 ppm) or Nb_2C-IO-CaO_2 nanosheets (50 ppm) at pH 7.4 or 6.5 for 12 h, with or without the irradiation of 1064 nm laser (1.0 W cm^{-2}), the cells were collected by centrifugation. Then, the cells were transferred into the test tube and stained by the Annexin V-FITC/PI Apoptosis Detection Kit (Dojindo Molecular Technologies, Inc., Japan) for 20 min for the flow cytometric apoptosis analysis.

17. Live/Dead (Calcein AM / PI) Cell Staining

4T1 cells were seeded (1×10^5 cells, 1 mL) in CLSM-exclusive culture dishes for 24 h to adhere. Then, the culture media were by fresh DMEM (pH 7.4 or 6.5) containing Nb_2C-IO-CaO_2 nanosheets (50 ppm). After incubation for 6 h, the culture medium was replaced by fresh DMEM medium, followed by irradiation for 5 min under 1064 nm laser at the power density of 1.0 W cm^{-2}. After rinsed with PBS for three times, Calcein-AM (100 μL) and PI solution (100 μL) were added and co-incubated with the cells for 15 min to stain the live and dead cells, respectively. Finally, the live cells with green fluorescence (λ_{ex} = 490 nm, λ_{em} = 515 nm) and dead cells with red fluorescence (λ_{ex} = 535 nm, λ_{em} = 617 nm) were visualized by CLSM.

18. Live subject statement

All animal experiments procedures were performed in compliance with the protocols approved by Institutional Animal Care and Use Committee (IACUC) and the care regulations approved by the administrative committee of laboratory animals of Fudan University.

19. *In Vivo* Toxicity Assessment

Twenty SPF-leveled healthy female Kunming mice (~ 22 g, four-week-old) were raised at Laboratory Animal Center, Shanghai Medical College of Fudan University. The mice were randomly divided into four groups (n = 5) subjected to intravenous (*i.v.*) administration of (1) saline (control group), Nb_2C-IO-CaO_2 nanosheets (100 μL, dosage: 20 mg kg^{-1}) for (2) 1 d, (3) 7 d and (4) 28 d. The mice body weights were measured every two days and histological analysis, hematological and blood biochemical indexes were collected at the given intervals.

20. Pharmacokinetics, Biodistribution and Metabolism Studies

Pharmacokinetic analysis: Healthy female Kunming mice (n = 3) were *i.v.* injected with Nb_2C-IO-CaO_2 nanosheets (100 μL, dosage: 20 mg kg^{-1}). At varied time points (2, 5, 8, 10, 15, 30 min, 1, 2, 4, 8, 12 and 24 h) post injection, 10 μL of blood was

collected for quantitative analysis of Nb element by ICP-OES. Origin software was used for data analysis for the best-fit line and blood terminal half-life based on the two-compartment pharmacokinetic model.

Biodistribution analysis: 4T1 xenografted tumor model was established on 4-week-old female Balb/c mice by subcutaneous (*s.c.*) injection of 4T1 cells (1×10^6 cell/site, 100 μL saline) into the left rear legs of mice. 4T1 tumor-bearing mice (n = 3) were *i.v.* injected with Nb_2C-IO-CaO_2 nanosheets (100 μL, dosage: 20 mg kg^{-1}). At predesignated time points (2, 4, 6, 12, 24 and 48 h) post injection, the tumor tissues and major organs were collected, weighed and digested in aqua regia for quantitative analysis of Nb element by ICP-OES. The Nb distribution in different tissues was calculated as the percentage of the original injected dosage per gram of tissue.

Metabolism analysis: 4T1 tumor-bearing mice (n = 3) were *i.v.* injected with Nb_2C-IO-CaO_2 nanosheets (100 μL, dosage: 20 mg kg^{-1}). At different time points (2, 4, 6, 12, 30 and 48 h) post injection, the urine and feces were collected and digested in aqua regia for quantitative analysis of Nb element by ICP-OES.

21. *In Vivo* Chemodynamic/Photothermal Therapy

To develop the 4T1 xenografted tumor model, 4T1 tumor cells (1×10^6 cell/site, 100 μL saline) were subcutaneously injected into the left rear legs of the 4-week-old female Balb/c mice (~ 15 g). Thirty-six 4T1 tumor-bearing mice (tumor volume ~50 mm^3) were randomly separated into six groups (n = 6) for various treatments including control (saline), laser only, Nb_2C-IO, Nb_2C-IO + laser, Nb_2C-IO-CaO_2, and Nb_2C-IO-CaO_2 + laser. The dosage of Nb_2C-IO or Nb_2C-IO-CaO_2 is 20 mg kg^{-1}. To conduct the *in vivo* PTT, all mice were anesthetized and irradiated with 1064 nm laser (1.0 W cm^{-2}, 10 min), with a thermal imaging camera monitoring the temperature change. The length (L) and width (W) of tumors were recorded by a digital caliper every two days during half a month post injection, and the tumor volume was calculated to be $L \times W^2/2$.

The tumor tissues were dissected 24 h after different treatments and sliced for hematoxylin and eosin (H&E), terminal deoxynucleotidyl transferase mediated dUTP

nick-end labeling (TUNEL) and Ki-67 antibody staining assay for histological analysis.

22. Statistical Analysis

Quantitative data are expressed as mean ± s.d. Statistical comparisons were conducted by using Student's two-sided t-test as $*P < 0.05$ (significant), $**P < 0.01$ (moderately significant) and $***P < 0.001$ (highly significant).

B: Supplementary Discussions

Discussion S1. *In vitro* catalytic Fenton reactivity and Michaelis-Menten kinetics of Nb_2C-IO nanosheets.

The ·OH-generating activity of Nb_2C-IO nanosheets was evaluated with extra-added H_2O_2 using the typical colorimetric assay established on TMB. The oxidation of oxTMB is significantly promoted at the elevated concentrations of both Nb_2C-IO (**Fig. S9**) and H_2O_2 (**Fig. S10**). Importantly, the steady-state catalytic kinetics of Nb_2C-IO was investigated at room temperature (25℃) in Na_2HPO_4-citric acid buffer solution (pH 6.5). The time-dependent absorbance variations of the reaction solution containing Nb_2C-IO, TMB and H_2O_2 of varying concentrations were monitored in time-scan mode at 652 nm using a microplate reader. At each H_2O_2 concentration (20, 30, 40, 50 mM), the concentration-changing rate (v) of oxTMB was obtained from the absorbance-changing rate according to the Beer-Lambert law, $A = \varepsilon lc$, where A is the absorbance, ε is the molar absorbance coefficient (39000 $M^{-1}cm^{-1}$ for oxTMB), l is the path length (10 mm), and c is the molar concentration of H_2O_2. The relationship between oxTMB concentration change rate and the corresponding H_2O_2 concentration follows the typical Michaelis-Menten equation (**Fig. S11a**), $v_0 = V_{max}[S] / (K_m + [S])$, where v_0 is the initial velocity of the reaction, V_{max} is the maximal velocity of reaction, [S] is the substrate (H_2O_2) concentration, and K_m is the Michaelis-Menten constant. According to the Lineweaver-Burk plot (**Fig. S11b**), the K_m and V_{max} values of the catalytic reaction by Nb_2C-IO were calculated to be 27.0 mM and 5.9×10^{-7} M s^{-1}, respectively. Furthermore, the temperature-dependent catalytic activity of Nb_2C-IO nanosheets was examined. The UV-vis absorbance at 652 nm of oxTMB shows an evident increase with the elevation of temperature, which indicates that the catalytic activity of Nb_2C-IO as the Fenton agent could be significantly enhanced by temperature elevation (**Fig. S12**). The electron spin resonance (ESR) spectroscopy was employed to *in situ* detect ·OH radicals with 5,5-dimethyl-1-pyrroline-N-oxide (DMPO) as the ·OH radical-specific detector, which features with the characteristic 1:2:2:1 signal (**Fig. S13**). The increased ESR signal intensity at pH 6.5 in comparison to that at pH 7.4 indicates that the enhanced yield of

·OH radicals and higher Fenton catalytic activity in acid condition than in neutral condition. It is noteworthy that, the enhanced ESR signal intensity at the elevated higher temperatures indicates the production of larger enlarged amounts of ·OH radicals, confirming the thermal-augmented effect on the catalytic Fenton reactivity.

Discussion S2. *In vivo* toxicity assessments

The *in vivo* toxicity assessments of Nb_2C-IO-CaO_2 nanosheets were conducted to guarantee their further potential clinical translation. Twenty SPF-leveled healthy female Kunming mice (~ 22 g, four-week-old) were randomly divided into four groups (n = 5) for intravenous (*i.v.*) administration of saline (control group), Nb_2C-IO-CaO_2 nanosheets (100 μL, dosage: 20 mg kg^{-1}) for 1 d, 7 d and 28 d. After intravenous (*i.v.*) administration of Nb_2C-IO-CaO_2 (100 μL, dosage: 20 mg kg^{-1}), no significant body-weight losses of mice were observed in 28 days post injection as compared to the control group (**Fig. S24**). The hematological and blood biochemical analysis were performed at time points of 1, 7 and 28 days post injection. The standard blood biochemical indexes and normal hematology parameters were then examined, including alanine transaminase (ALT), aspartate transaminase (AST), alkaline phosphatase (ALP), blood urea nitrogen (BUN), creatinine (CREA), white blood cells (WBC), red blood cells (RBC), hemoglobin (HGB), mean corpuscular volume (MCV), mean corpuscular hemoglobin (MCH), mean corpuscular hemoglobin concentration (MCHC), platelets (PLT) and hematocrit (HCT). All these indexs in mice treated with Nb_2C-IO-CaO_2 nanosheets in the groups of 1 day, 7 days and 28 days show no significant changes as compared to those in the control group (**Fig. S25**), which implys that Nb_2C-IO-CaO_2 nanosheets injected at the dosage of 20 mg kg^{-1} induce no significant negative impact on the major blood indexes. The major organs were harvested and sliced for histological analysis by hematoxylin and eosin (H&E) staining (**Fig. S26**). The stained tissue sections (heart, liver, spleen, lung and kidney) in groups injected with Nb_2C-IO-CaO_2 nanosheets for 1 day, 7 days and 28 days demonstrate no histological abnormalities compared to the control group, implying no significant acute

and chronic pathological toxicity of Nb_2C-IO-CaO_2. These results indicate the high biosafety and biocompatibility of Nb_2C-IO-CaO_2 nanosheets, which is beneficial for further *in vivo* therapeutic applications.

C：Supplementary Figures

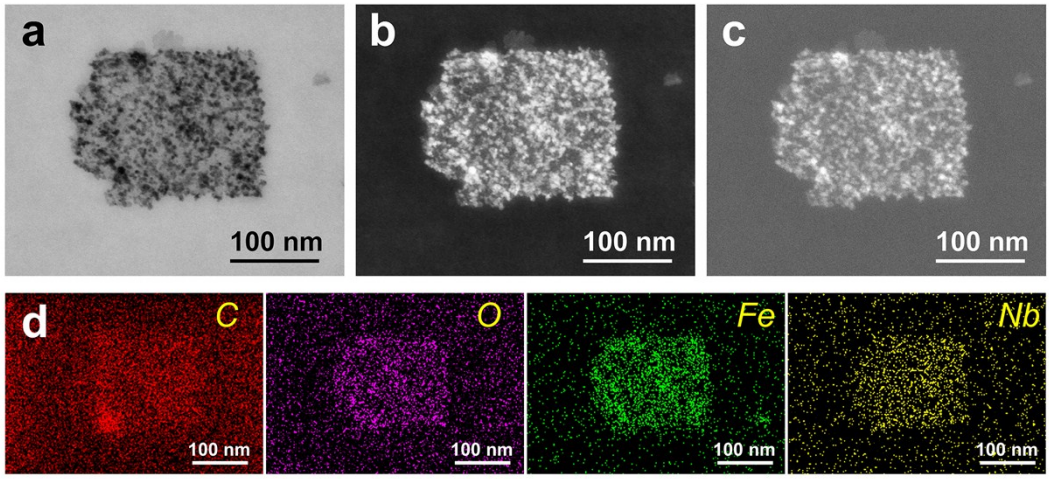

Fig. S1 (a) Bright-field STEM image, (b) SEM image, (c) High-Angle Annular Dark Field (HAADF)-STEM image and (d) corresponding element mappings (for C, O, Fe, and Nb) of Nb_2C-IO composite nanosheets.

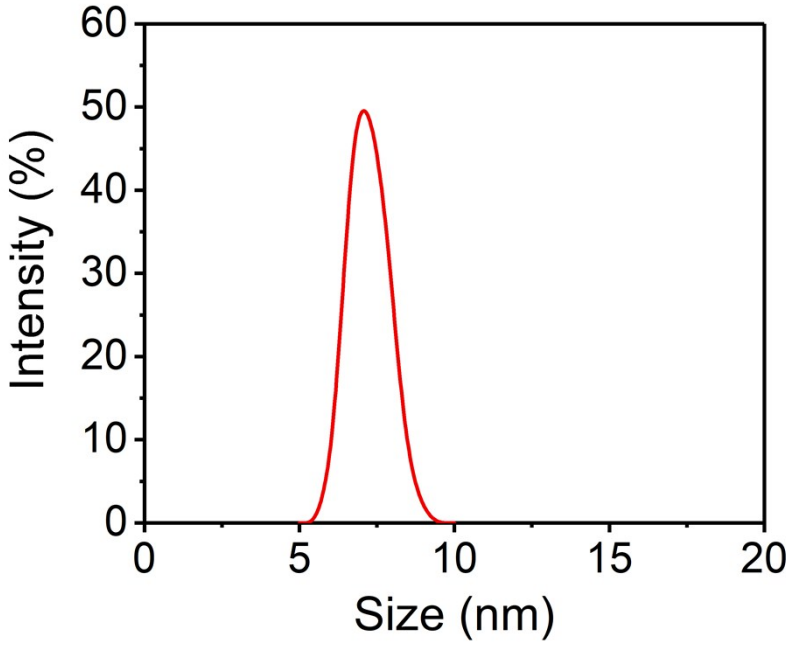

Fig. S2 Particle-size distribution of CaO_2 NPs dispersed in water as tested by dynamic light scattering (DLS).

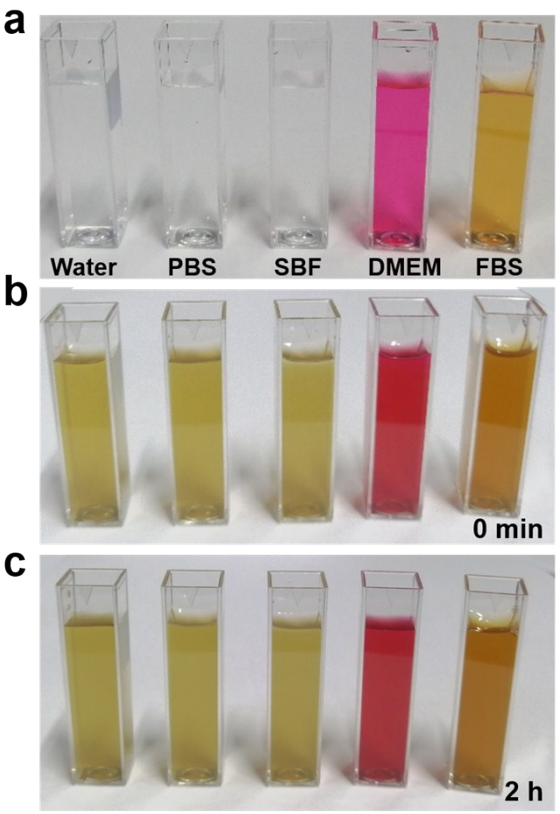

Fig. S3 (a) Digital photographs of water, PBS, SBF, DMEM and FBS. Digital photographs of the Nb_2C-IO-CaO_2 composite nanosheets after dispersed in the above solutions for (b) 0 min and (c) 2 h.

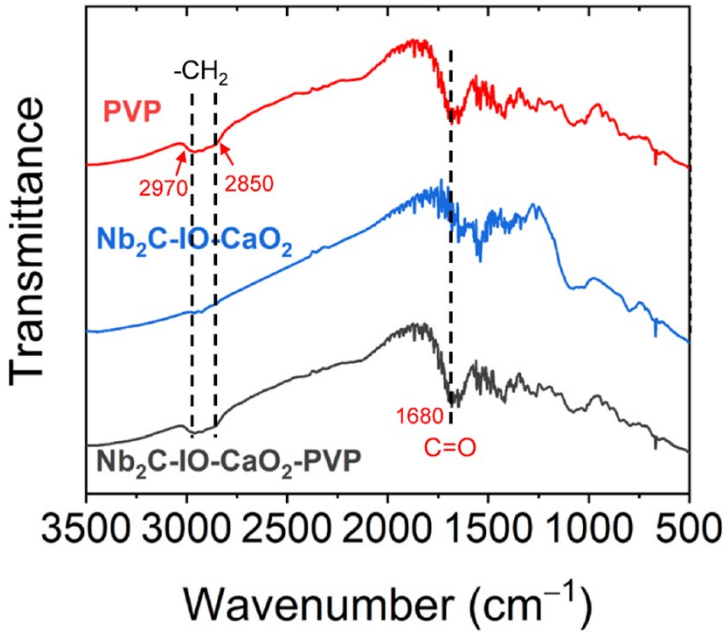

Fig. S4 FTIR spectra of PVP, Nb_2C-IO-CaO_2 and Nb_2C-IO-CaO_2-PVP nanosheets.

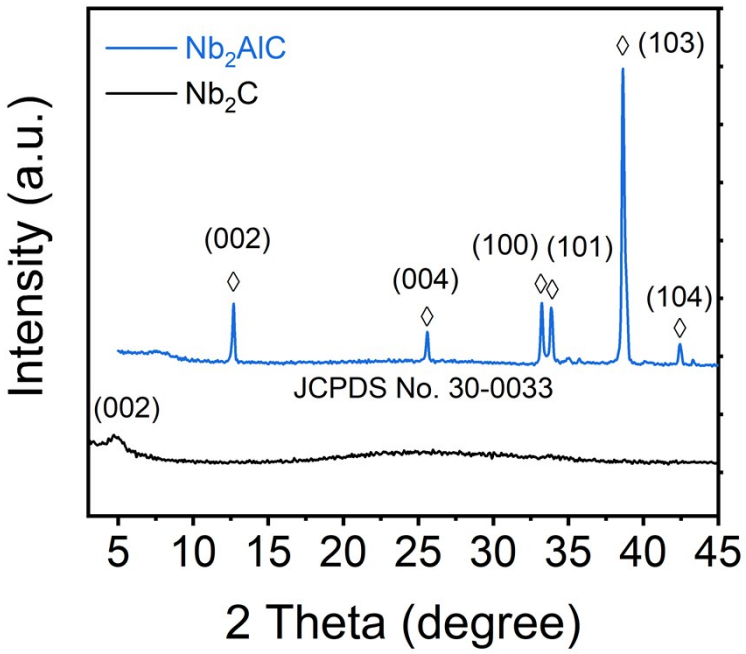

Fig. S5 XRD patterns of the Nb_2AlC powder and Nb_2C nanosheets.

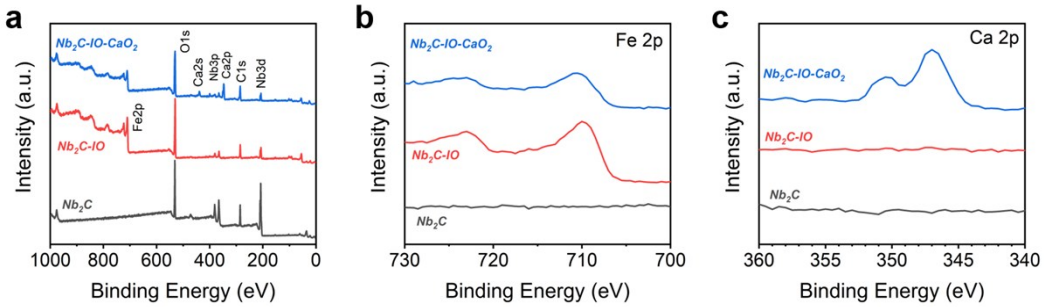

Fig. S6 (a) XPS survey spectra, (b) Fe 2p and (c) Ca 2p core level spectra of Nb_2C, Nb_2C-IO and Nb_2C-IO-CaO_2.

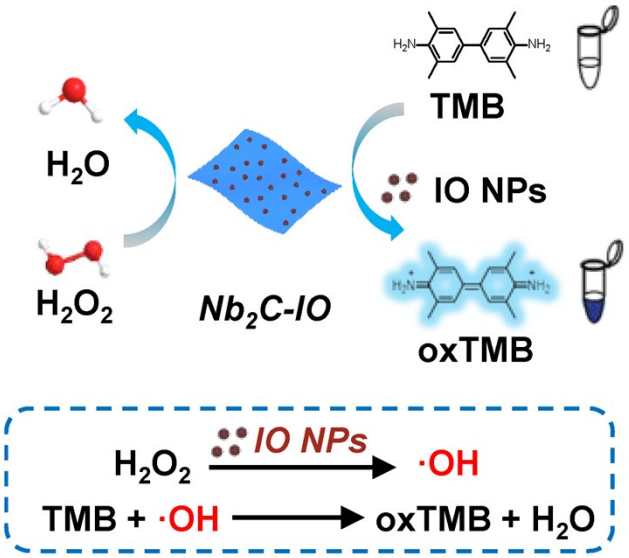

Fig. S7 Schematic illustration of Nb_2C-IO nanosheets-catalyzed TMB oxidation reaction with exogenous H_2O_2.

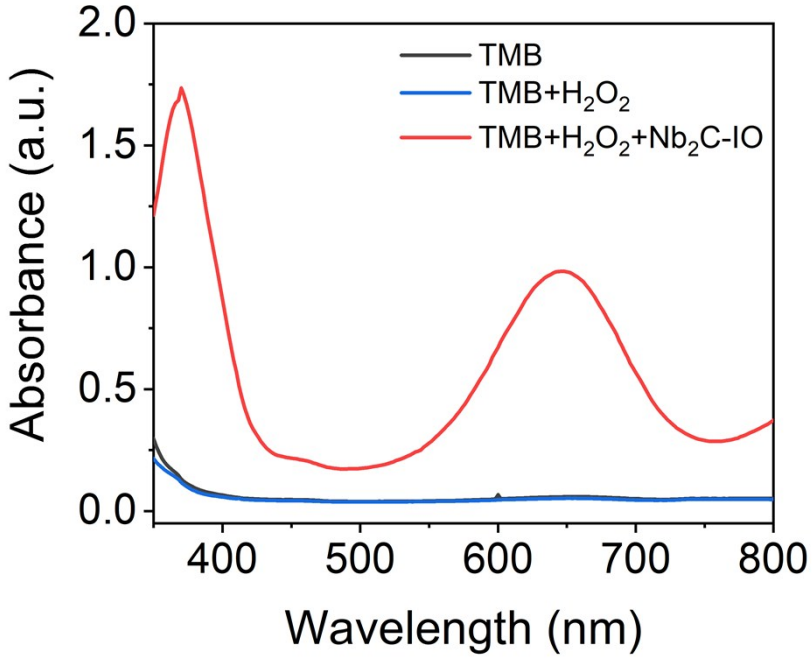

Fig. S8 UV-vis absorption spectra of TMB, TMB + H_2O_2 and TMB + H_2O_2 + Nb_2C-IO in the reaction buffer (pH 6.5) after 30 min incubation.

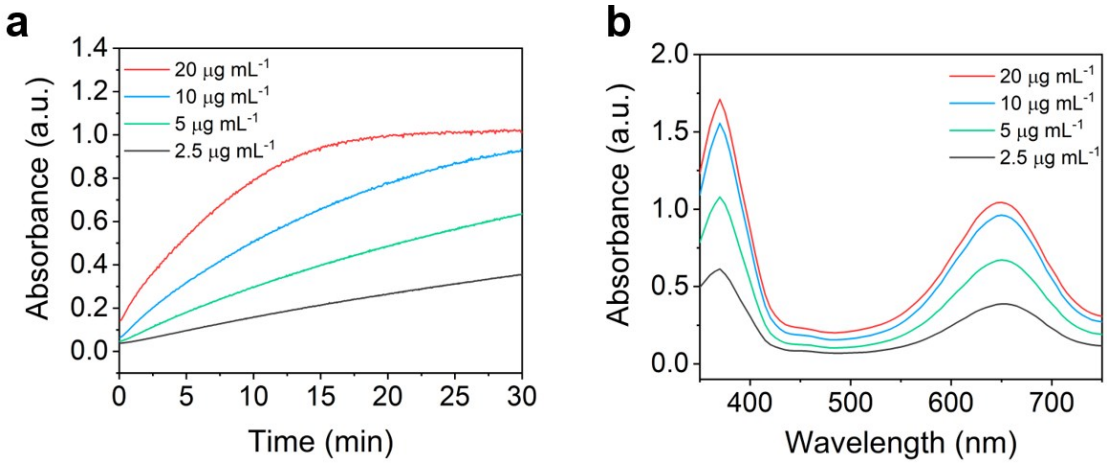

Fig. S9 (a) Time-dependent absorbances at 652 nm of TMB incubated with H_2O_2 and Nb_2C-IO at varied concentrations (2.5, 5, 10, 20 μg mL^{-1}) in the reaction buffer (pH 6.5). (b) UV-vis absorption spectra of TMB as catalyzed by H_2O_2 and Nb_2C-IO at varied concentrations (2.5, 5, 10, 20 μg mL^{-1}) at pH 6.5 after reaction for 30 min.

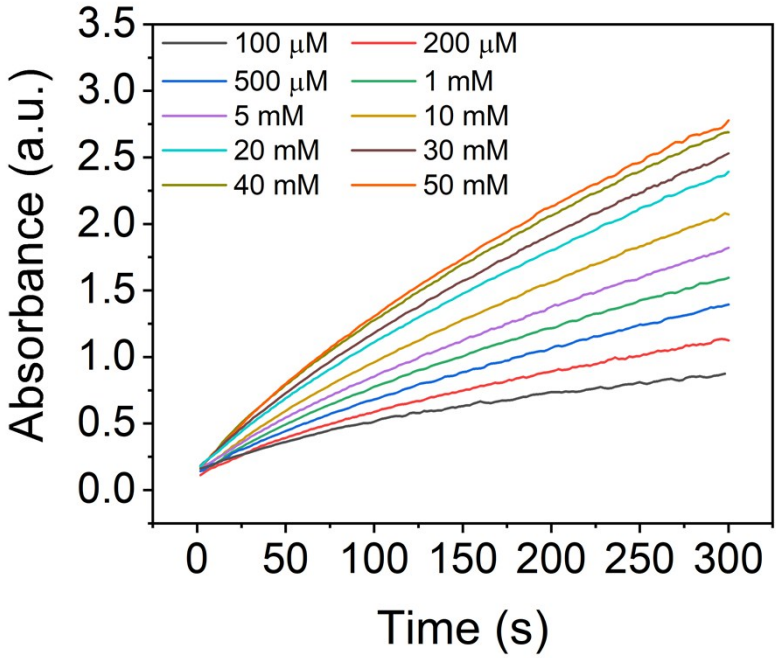

Fig. S10 Time-dependent absorbances at 652 nm of TMB as catalyzed by Nb_2C-IO and H_2O_2 at different concentrations (100, 200, 500 μM, 1, 5, 10, 20, 30, 40, 50 mM) in the reaction buffer (pH 6.5).

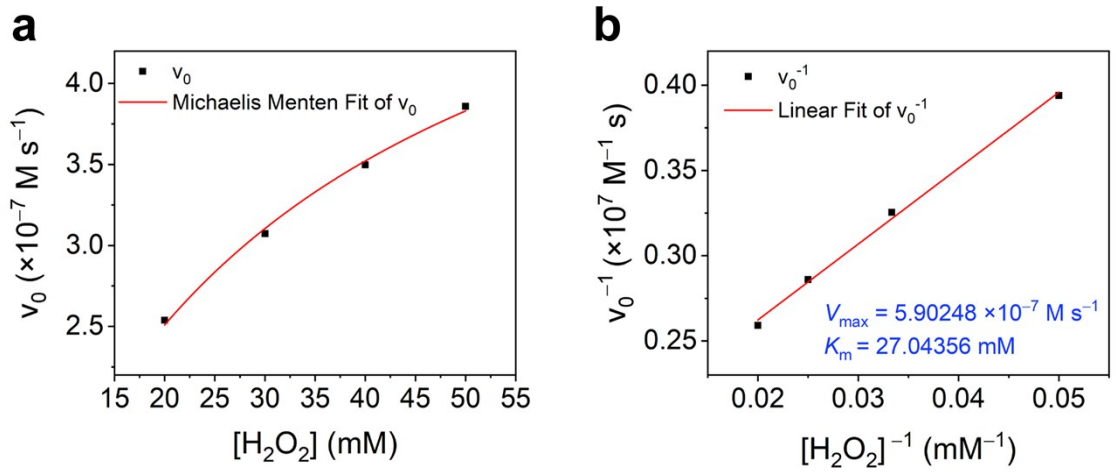

Fig. S11 (a) Michaelis-Menten kinetic analysis and (b) Lineweaver-Burk plotting for Nb_2C-IO with H_2O_2 as substrate. The initial reaction velocity (v_0) was calculated from the initial slopes of absorbance *vs.* time plots in Fig. S7.

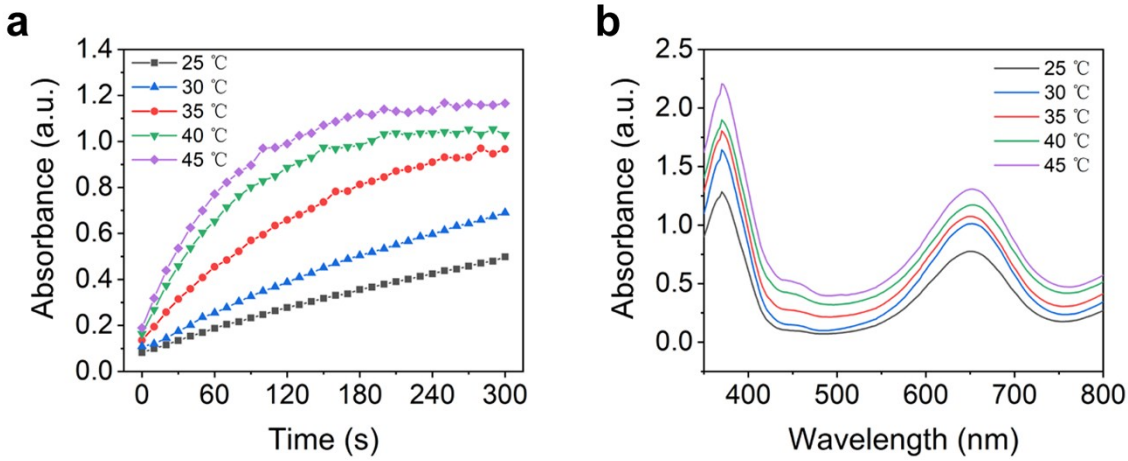

Fig. S12 (a) Time-dependent absorbances at 652 nm of TMB incubated with H_2O_2 and Nb_2C-IO at varied temperatures (25, 30, 35, 40, and 45℃) at pH 6.5. (b) UV-vis absorption spectra of TMB as catalyzed by H_2O_2 and Nb_2C-IO at varied temperatures (25, 30, 35, 40, and 45℃) at pH 6.5 after reaction for 10 min.

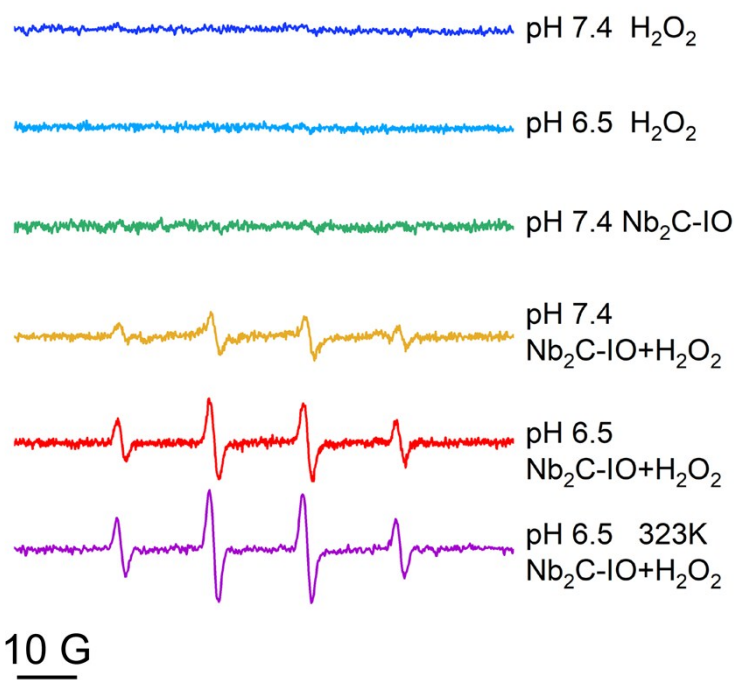

Fig. S13 ESR spectra of DMPO in the reaction buffer as catalyzed by Nb_2C-IO-CaO_2 in different conditions.

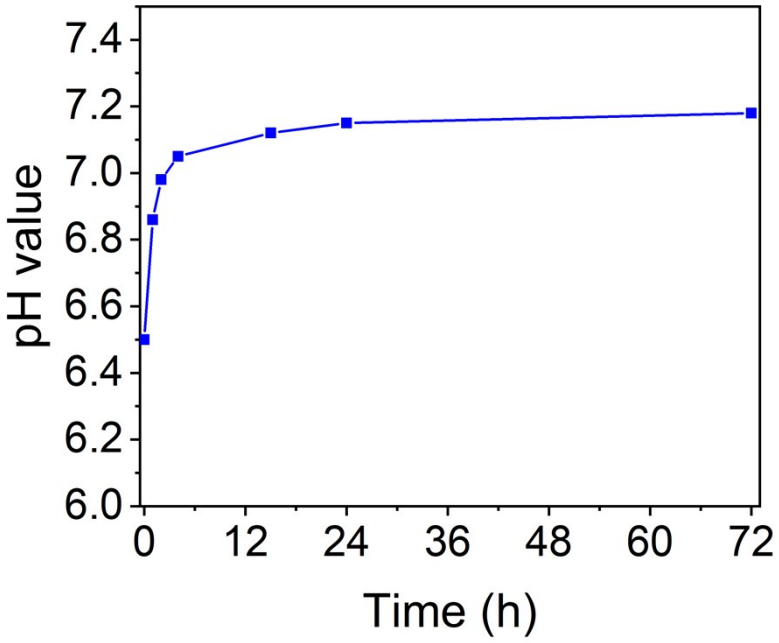

Fig. S14 The pH value change of the reaction buffer containing CaO_2 NPs over time.

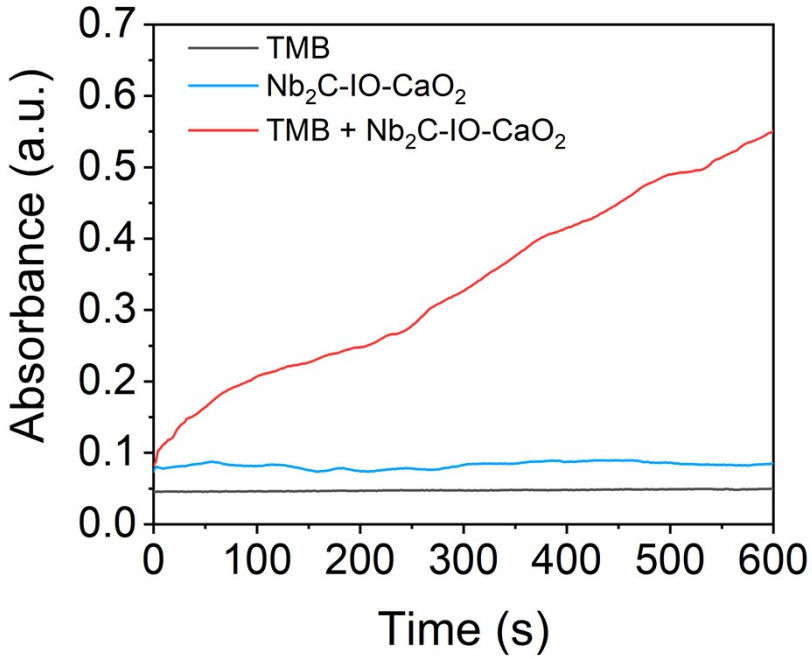

Fig. S15 Time-dependent UV-vis absorbances of TMB, Nb_2C-IO-CaO_2 and TMB + Nb_2C-IO-CaO_2 at pH 6.5.

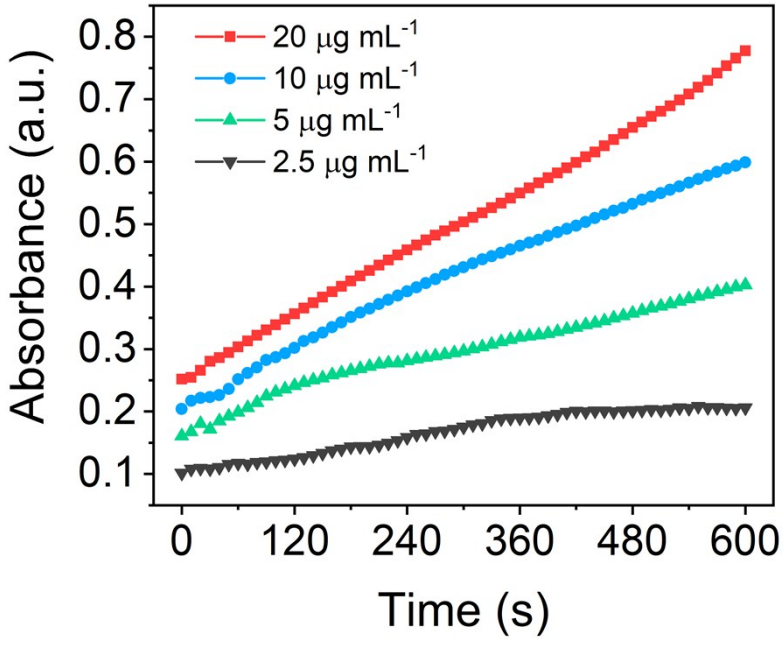

Fig. S16 Time-dependent UV-vis absorbances of TMB as catalyzed by Nb_2C-IO-CaO_2 of varied concentrations (2.5, 5, 10, 20 μg mL^{-1}) at pH 6.5.

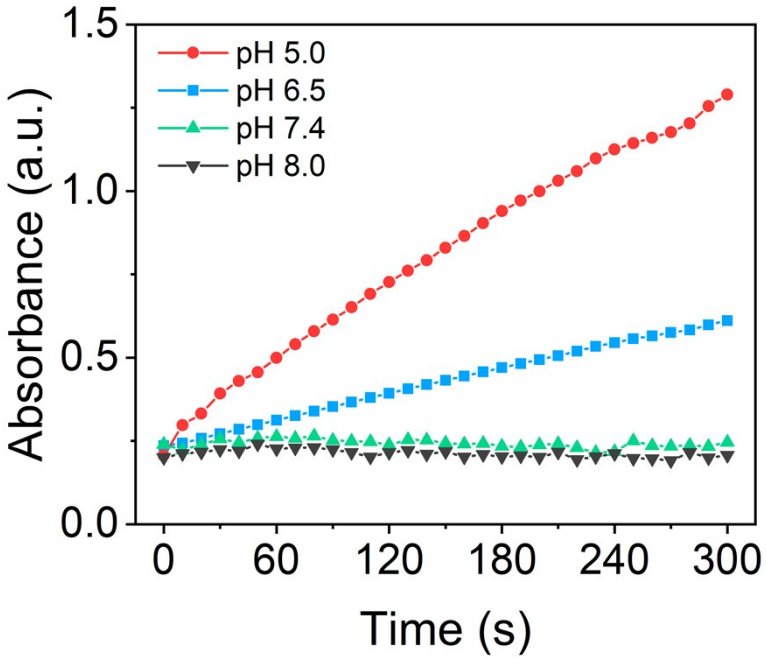

Fig. S17 Time-dependent UV-vis absorbances of TMB as catalyzed by Nb_2C-IO-CaO_2 at varied pH values of 5.0, 6.5, 7.4, and 8.0.

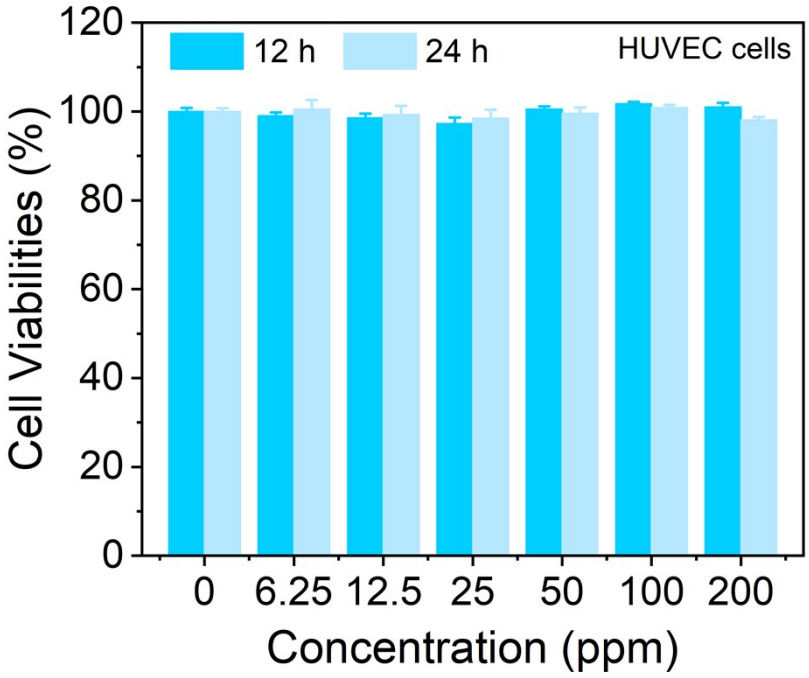

Fig. S18 Relative viabilities of HUVEC cells after incubated with Nb_2C-IO-CaO_2 at varied concentrations (0, 6.25, 12.5, 25, 50, 100, and 200 ppm) for 12 h and 24 h.

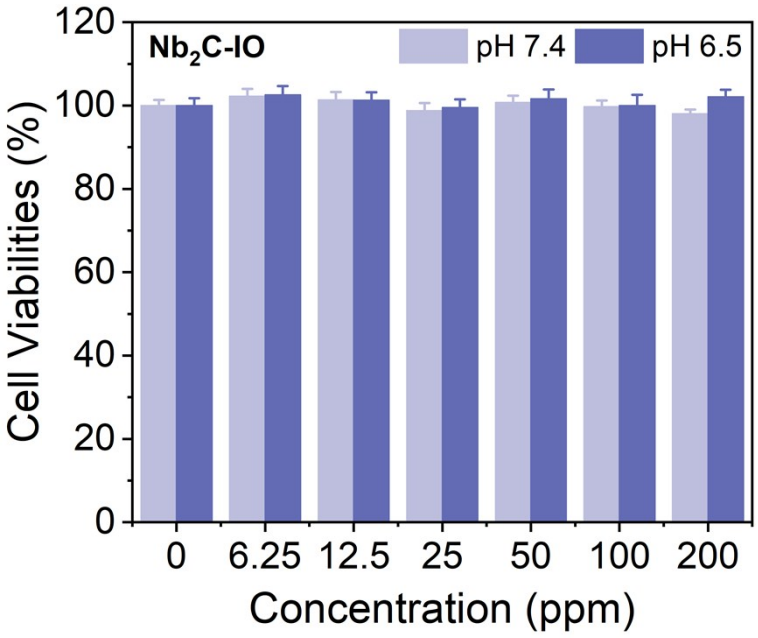

Fig. S19 Relative viabilities of 4T1 cells after incubated with Nb_2C-IO at varied concentrations (0, 6.25, 12.5, 25, 50, 100 and 200 ppm) at pH 7.4 and pH 6.5 for 24 h.

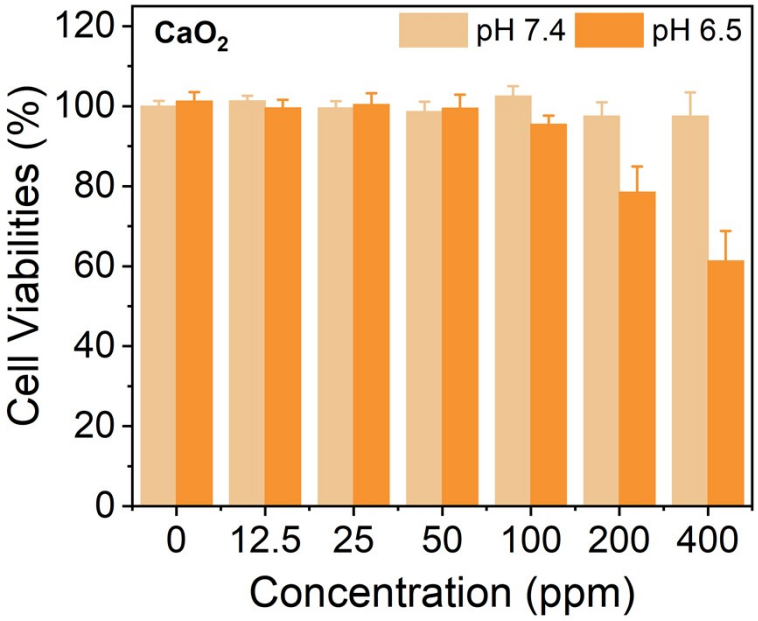

Fig. S20 Relative viabilities of 4T1 cells after incubated with CaO_2 NPs at varied concentrations (0, 12.5, 25, 50, 100, 200 and 400 ppm) at pH 7.4 and pH 6.5 for 24 h.

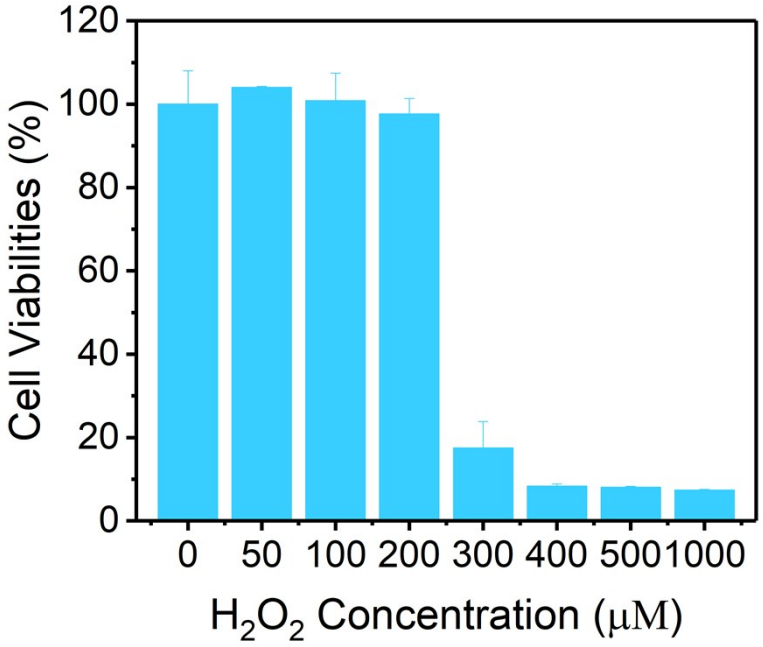

Fig. S21 Relative viabilities of 4T1 cells after incubated with H_2O_2 at varied concentrations (0, 50, 100, 200, 300, 400, 500 and 1000 μM) for 24 h.

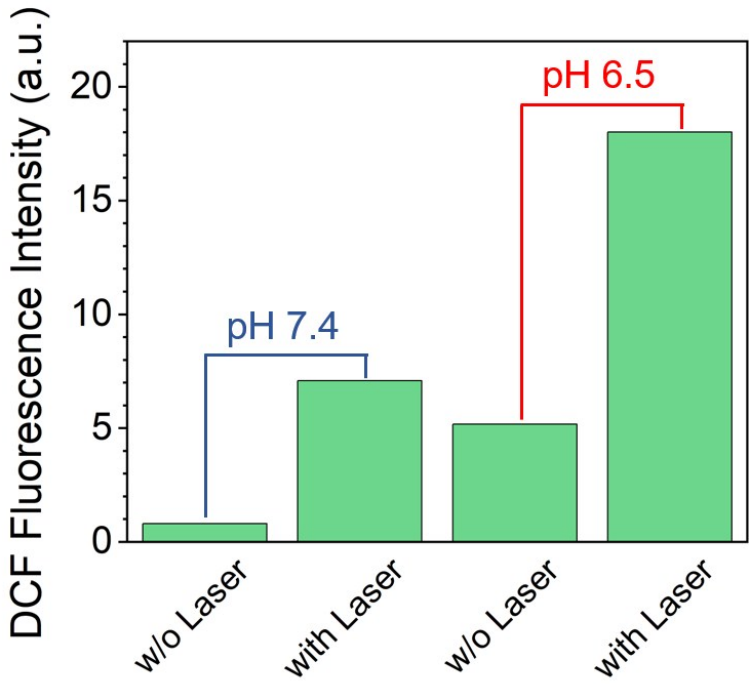

Fig. S22 DCF fluorescence intensity of DCFH-DA stained 4T1 cells after incubated with Nb_2C-IO-CaO_2 at pH 7.4 and 6.5 with or without 1064 nm laser irradiation.

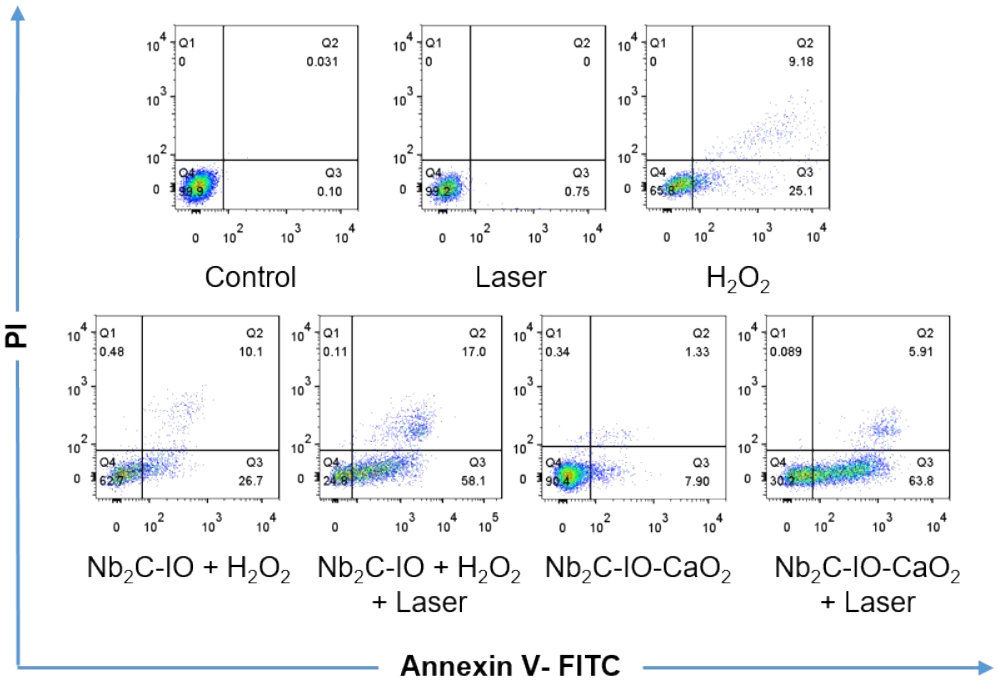

Fig. S23 Flow cytometric apoptosis analysis of Annexin V-FITC/PI strained 4T1 cells after different treatments at pH 7.4.

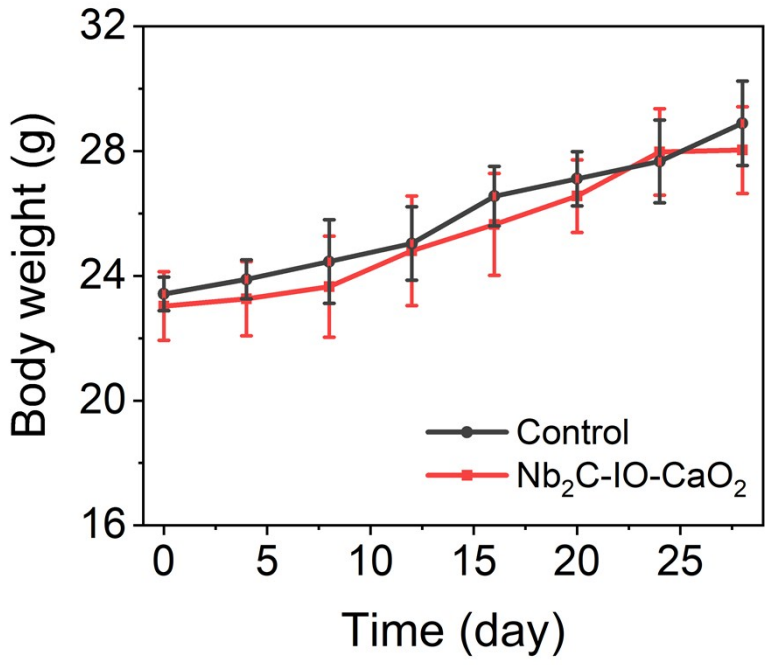

Fig. S24 Time-dependent body weight curves of healthy Kunming mice in 28 days after *i.v.* injection of Nb_2C-IO-CaO_2 nanosheets.

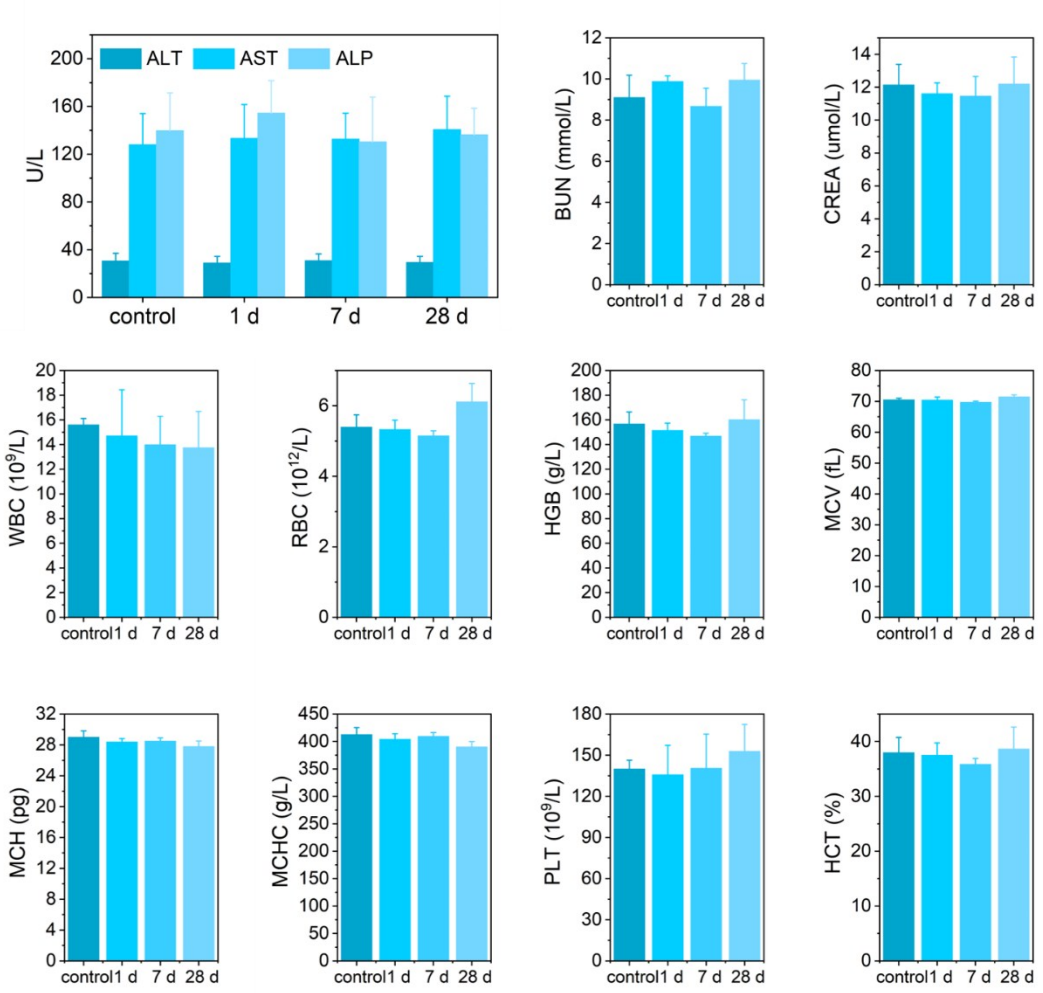

Fig. S25 Hematological and blood biochemical analyses of Kunming mice injected with Nb_2C-IO-CaO_2 in 1, 7 and 28 days post injection.

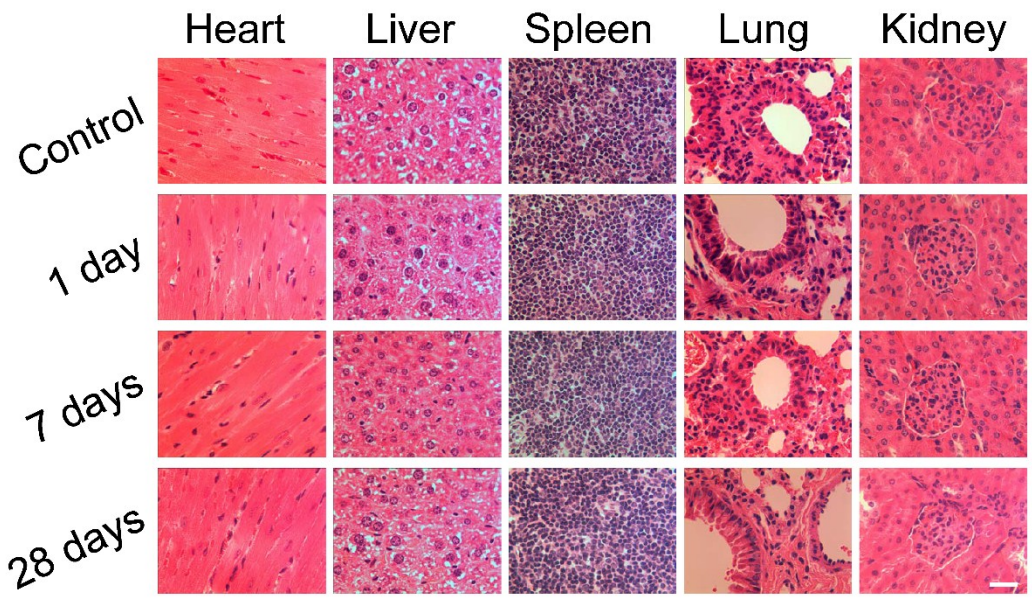

Fig. S26 Histological assessments for the major organs (heart, liver, spleen, lung and kidney) of Kunming mice after treatment with Nb_2C-IO-CaO_2 in 1, 7 and 28 days post-injection. Scale bar: 50 μm.

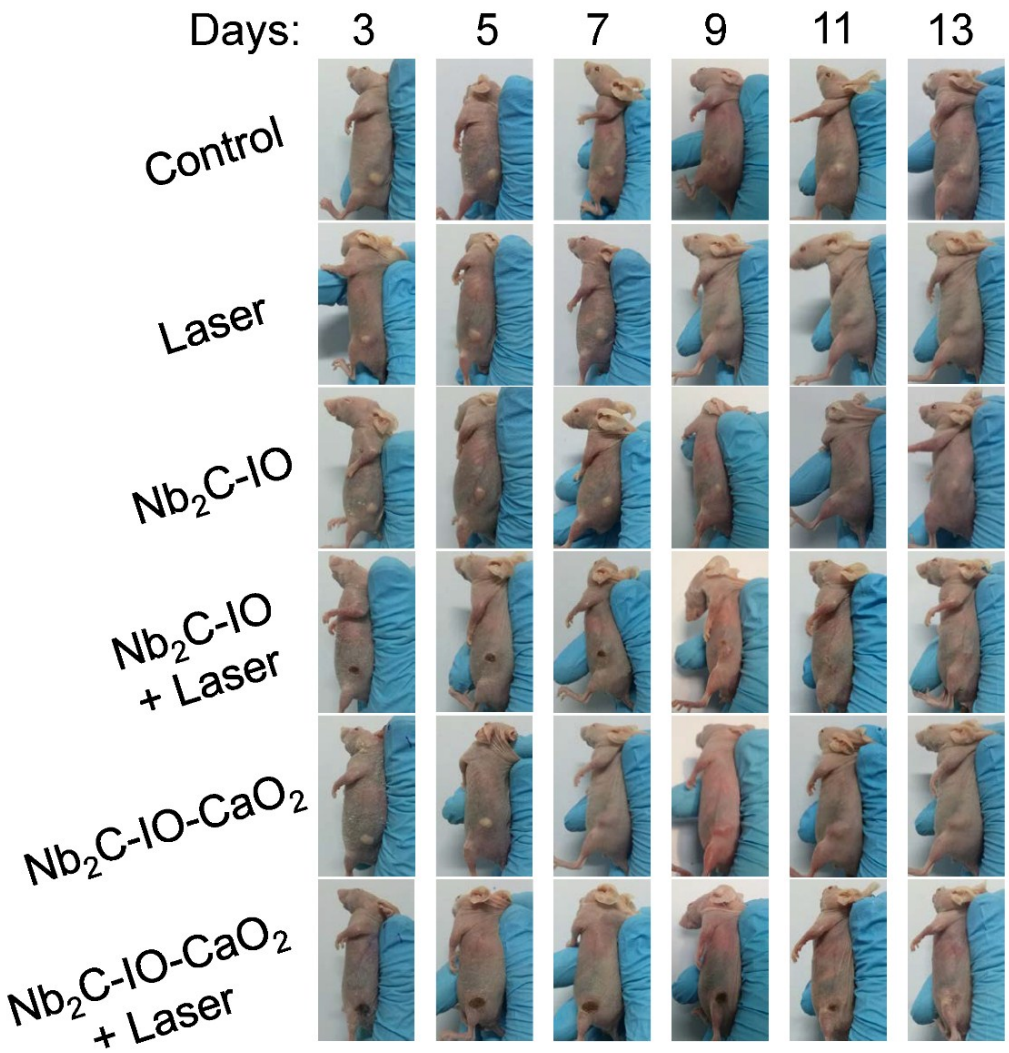

Fig. S27 Photographs of 4T1 tumor-bearing mice after different treatments during the therapeutic period.

D：Supplementary Tables

Element	Nb (ppm)	Fe (ppm)	Ca (ppm)	Atom ratio
Nb_2C-IO-CaO_2	201.04	82.36	150.68	Nb:Fe:Ca = 1:0.41:0.75
Nb_2C-IO	271.37	116.84	/	Nb:Fe = 1:0.43

Table S1 The concentration of Nb, Fe and Ca elements and the corresponding atom ratio of Nb_2C-IO and Nb_2C-IO-CaO_2 as measured by ICP experiment (n = 3).

References

1. S. Zhang, X. Zhao, H. Niu, Y. Shi, Y. Cai and G. Jiang, *J. Hazard. Mater.*, 2009, **167**, 560-566.
2. R. A. Bini, R. F. C. Marques, F. J. Santos, J. A. Chaker and M. Jafelicci, *Journal of Magnetism and Magnetic Materials*, 2012, **324**, 534-539.
3. D. K. Roper, W. Ahn and M. Hoepfner, *J. Phys. Chem. C*, 2007, **111**, 3636-3641.